

Supporting Information: Fast and Accurate Electronic Excitations in Cyanines with the Many-Body Bethe-Salpeter Approach

Paul Boulanger,[†] Denis Jacquemin,^{*,‡,¶} Ivan Duchemin,[§] and Xavier Blase^{*,||,||,†}

*CNRS, Inst NEEL, F-38042 Grenoble, France, Laboratoire CEISAM - UMR CNRS 6230,
Université de Nantes, 2 Rue de la Houssinière, BP 92208, 44322 Nantes Cedex 3, France, Institut
Universitaire de France, 103, bd Saint-Michel, F-75005 Paris Cedex 05, France., INAC,
SP2M/L_Sim, CEA/UJF Cedex 09, 38054 Grenoble, France, and Univ. Grenoble Alpes, Inst
NEEL, F-38042 Grenoble, France*

E-mail: denis.jacquemin@univ-nantes.fr; xavier.blase@neel.cnrs.fr

S1 GW/BSE excitation energies

For completeness, we give in Table S-I and Table S-II the full results of the GW and BSE calculations which are used in the generation of the two main figures. Results were obtained with the aug-cc-pVTZ basis,¹ the auxiliary basis presented below and using all virtual orbitals for the generation of the BSE matrix. Notice that the COHSEX column here corresponds to the BSE/GW results in Figure 1 and 2.

*To whom correspondence should be addressed

[†]CNRS

[‡]CEISAM, Nantes

[¶]IUF, Paris

[§]INAC

^{||}Univ.Grenoble

Table S-I: Results (in eV) for self-consistent GW on the eigenvalue with selected input wavefunctions.

	GW IP			GW EA			GW Gap		
	PBE	COHSEX	HF	PBE	COHSEX	HF	PBE	COHSEX	HF
CN5	-13.60	-13.39	-14.18	-4.02	-3.76	-4.26	9.58	9.63	9.92
CN7	-11.83	-11.78	-12.45	-4.29	-4.13	-4.54	7.54	7.64	7.90
CN9	-10.70	-10.67	-11.34	-4.40	-4.24	-4.64	6.29	6.44	6.70
CN11	-9.88	-9.91	-10.59	-4.45	-4.33	-4.72	5.43	5.58	5.87

Also included in Table S-II are the oscillator strengthes (f) for the different cyanines. All methods predict an increase of the oscillator strength with the chain length and a decrease with the amount of exact-exchange included in the functional used to generate the "frozen" input wavefunctions.

Table S-II: GW/BSE values for the first singlet excitation of the cyanines. All energies are in eV.

	Excitation Energy					Oscillator Strength				
	COHSEX	PBE	B3LYP	HBLYP	HF	COHSEX	PBE	B3LYP	HBLYP	HF
CN5	4.80	4.99	4.94	4.91	4.94	0.47	0.56	0.53	0.49	0.42
CN7	3.63	3.83	3.78	3.75	3.67	0.74	0.92	0.85	0.75	0.61
CN9	2.96	3.15	3.11	3.07	2.96	1.00	1.30	1.18	1.01	0.78
CN11	2.48	2.71	2.66	2.61	2.49	1.24	1.72	1.52	1.26	0.93

S2 Convergence with respect to the KS basis

Investigating the effect of the underlying basis set on the **CN5** molecule, we can readily see in Table S-III that augmentation is crucial to obtain tightly converged results for the excitation energies, while the oscillator strengths are rather impervious, except for the smallest cc-pvdz basis. The aug-cc-pvtz basis leads to an error of ca. 6 meV when compared with aug-cc-pvqz basis.

S3 Convergence with respect to the auxiliary basis

The use of resolution of the identity techniques is one of the strategies employed by the FIESTA package^{2,3} to increase the efficiency of the calculations. In this case, we have opted for the more

Table S-III: BSE first singlet excitation energy (in eV) and oscillator strength.

	Excitation energy		Oscillator Strength	
	cc-pVXZ	aug-cc-pVXZ	cc-pVXZ	aug-cc-pVXZ
X=D	5.17	4.92	0.53	0.49
X=T	4.96	4.82	0.49	0.48
X=Q	4.87	4.81	0.49	0.47

accurate, albeit more costly, resolution of the identity with the Coulomb metric (RI-V), involving two-electron three-center Coulomb integrals. The resulting auxiliary basis depends on the underlying KS basis since it strives to accurately represent the KS product basis. To do so, we have chosen an even-tempered scheme,⁴ which scale the gaussian exponents (α) as:

$$\alpha_i = \alpha_{min} * \left(\frac{\alpha_{max}}{\alpha_{min}} \right)^{\frac{i-1}{N-1}} \quad (\text{S-1})$$

where N is the maximum number of primitive gaussians per angular momentum channel. The minimum exponent (α_{min}), a.k.a. most diffuse gaussian, is chosen to be the same as in the KS basis. The maximum exponent (α_{max}), the number of gaussians (N) and the maximum angular channel (l_{max}) are determined by converging the BSE values.

The variation of the BSE results on the auxiliary basis set used in conjunction with the aug-cc-pvtz KS basis is displayed in Figure S-1 and Figure S-2 for **CN5**. For brevity, only the convergence with respect to the carbon auxiliary basis is shown, but similar results are found for nitrogen. In Figure S-1 we can see that in order to obtain a precision comparable with the KS basis (ca. 6 meV), α_{max} must be greater than 8000 (which corresponds to the maximum exponent in the aug-cc-pVTZ basis). Hence, we have conservatively chosen $\alpha_{max} = 16000$ (the maximum value of the product basis). As for the oscillator strengths, they are once again easier to converge (variations of the order of 0.001).

Similarly, in Figure S-2 we see that 8 gaussians per channel are necessary to obtain a level of accuracy similar to the one obtained with the KS basis (ca. 6 meV). Finally, we have chosen $l_{max} = 2$ which leads to errors of 30 meV when compared with $l_{max} = 3$ (this error is visible when comparing results from Figure S-2 which include the f-channel and Table S-III which does not).

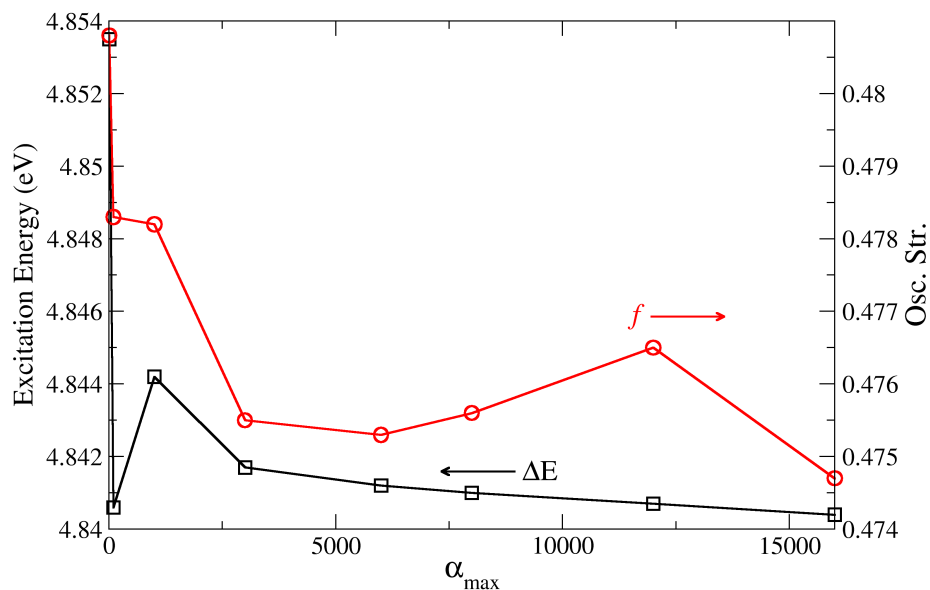


Figure S-1: Lowest singlet excitation energy (ΔE) and oscillator strength (f) for **CN5** as a function of the maximal exponent of the primitive gaussians in the auxiliary basis set. Notice that 16000 corresponds to the maximum of the product basis.

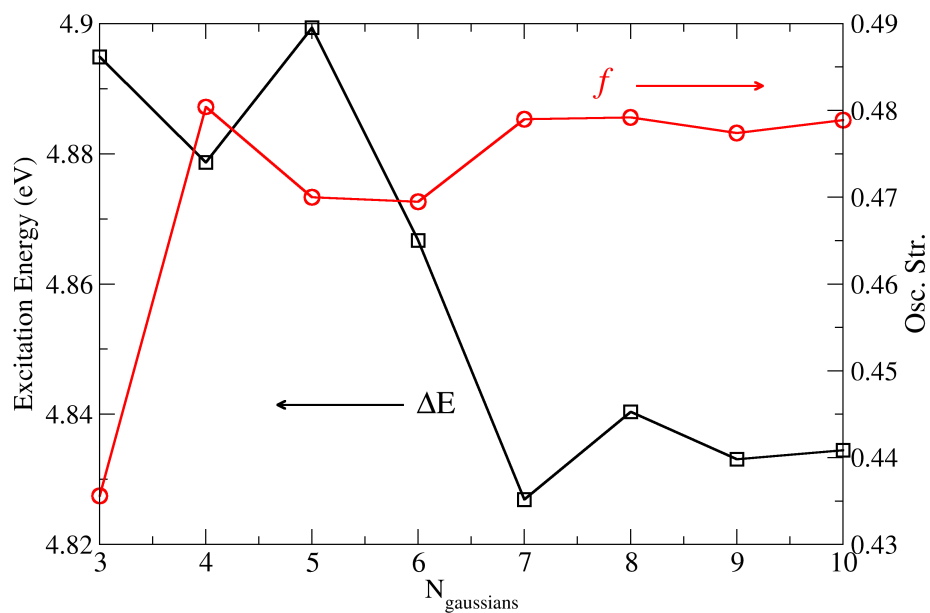


Figure S-2: Lowest singlet excitation energy (ΔE) and oscillator strength (f) for **CN5** as a function of the number of primitive gaussians per angular momentum channel.

Notice that the inclusion of an f-channel tends to slightly improve the agreement between GW/BSE and exCC3 for **CN5**. The auxiliary basis sets used in this study are included in section Section S7

S4 Convergence with respect to the number of virtual states included in the BSE active subspace

Even though we have used all virtual orbitals ($N_{virtual}$), it is interesting to look at the convergence of the BSE values with respect to the $N_{virtual}$ orbitals included in the construction of excitations and disexcitations in equation 9. As can be seen from Figure S-3 for **CN5**, the lowest singlet excitation energy and its related oscillator strength decrease monotonically with the number of states. The results can be already considered converged at 200 states, with a variation of 10 meV for the transition energy and 0.002 for the oscillator strength.

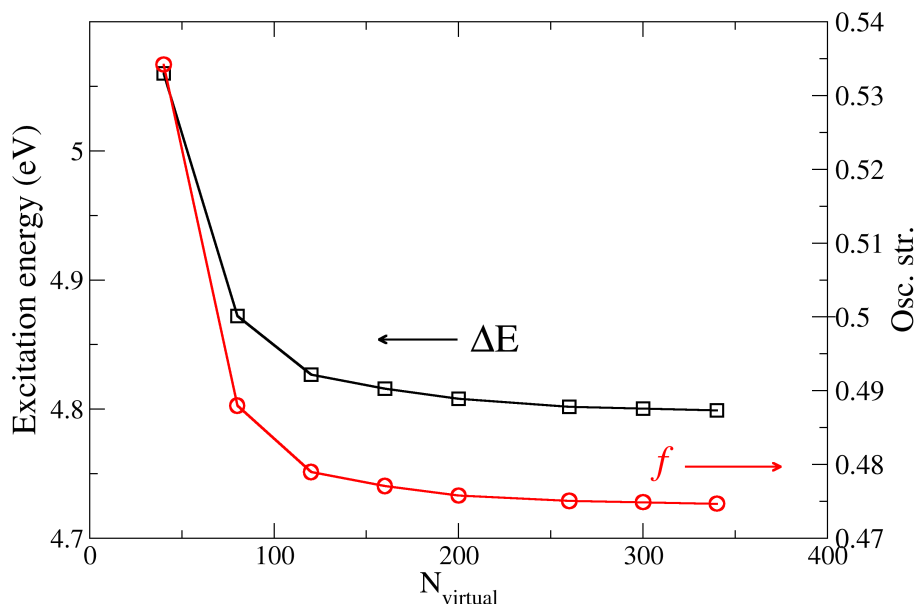


Figure S-3: Lowest singlet excitation energy (ΔE) and oscillator strength (f) for **CN5** as a function of the number of virtual orbitals included in the construction of excitation and disexcitation vectors. $N_{virtual} = 340$ is the total number of virtual states for **CN5** in the aug-cc-pVTZ basis.

S5 Effects of the Tamm-Dancoff approximation on *GW*/BSE excitation energies

Previous studies⁵ have shown that the Tamm-Dancoff approximations (TDA) to the standard TD-DFT formalism leads to large errors for the model cyanines. For convenience, the error induced in PBE0 TD-DFT calculations from Ref. 5 is reported in Table Table S-IV. In the case of BSE, the TDA is found, as expected, to yield similar large errors. with both methods, the TDA error on the excitation energy decreases slowly with chain length. On the contrary, the error associated to the oscillator strength is seen to increase rapidly.

Table S-IV: Tamm-Dancoff shifts for the PBE0 TD-DFT⁵ and *GW*@BSE excitations energies (in eV) and modification of the oscillator strengthes.

	PBE0 TD-DFT	<i>GW</i> @BSE	
	ΔE	ΔE	f
CN5	0.62	0.46	0.0048
CN7	0.60	0.47	0.0502
CN9	0.58	0.45	0.1078
CN11	0.56	0.42	0.1645

S6 Cartesian coordinates for the model cyanines

PBE0/cc-pVQZ geometry of the cyanines used here.⁵

Table S-V: Cartesian coordinates (in Å) for **CN5**.

	X	Y	Z
C	0.000000	0.000000	0.340620
C	0.000000	1.188118	-0.363814
C	0.000000	-1.188118	-0.363814
H	0.000000	0.000000	1.424526
H	0.000000	1.160197	-1.449153
H	0.000000	-1.160197	-1.449153
N	0.000000	2.389122	0.164413
N	0.000000	-2.389122	0.164413
H	0.000000	2.531432	1.161940
H	0.000000	-2.531432	1.161940
H	0.000000	3.211384	-0.414923
H	0.000000	-3.211384	-0.414923

Table S-VI: Cartesian coordinates (in Å) for **CN7**.

	X	Y	Z
C	0.000000	0.000000	0.258703
H	0.000000	0.000000	1.346928
C	0.000000	1.233147	-0.373850
C	0.000000	-1.233147	-0.373850
H	0.000000	1.288014	-1.456977
H	0.000000	-1.288014	-1.456977
C	0.000000	2.393799	0.371447
C	0.000000	-2.393799	0.371447
H	0.000000	2.327889	1.454856
H	0.000000	-2.327889	1.454856
N	0.000000	3.618036	-0.116310
N	0.000000	-3.618036	-0.116310
H	0.000000	3.790846	-1.108170
H	0.000000	-3.790846	-1.108170
H	0.000000	4.419815	0.489308
H	0.000000	-4.419815	0.489308

Table S-VII: Cartesian coordinates (in Å) for **CN9**.

	X	Y	Z
C	0.000000	0.000000	0.451338
H	0.000000	0.000000	1.536359
C	0.000000	1.207990	-0.224465
C	0.000000	-1.207990	-0.224465
H	0.000000	1.170185	-1.312049
H	0.000000	-1.170185	-1.312049
C	0.000000	2.465274	0.368365
C	0.000000	-2.465274	0.368365
H	0.000000	2.550740	1.449846
H	0.000000	-2.550740	1.449846
C	0.000000	3.602804	-0.405932
C	0.000000	-3.602804	-0.405932
H	0.000000	3.507917	-1.487016
H	0.000000	-3.507917	-1.487016
N	0.000000	4.844304	0.048913
N	0.000000	-4.844304	0.048913
H	0.000000	5.043211	1.035192
H	0.000000	-5.043211	1.035192
H	0.000000	5.628266	-0.578359
H	0.000000	-5.628266	-0.578359

Table S-VIII: Cartesian coordinates (in Å) for **CN11**

	X	Y	Z
C	0.000000	0.000000	0.153078
C	0.000000	1.232759	-0.484694
C	0.000000	-1.232759	-0.484694
C	0.000000	2.419726	0.221500
C	0.000000	-2.419726	0.221500
C	0.000000	3.695049	-0.339907
C	0.000000	-3.695049	-0.339907
C	0.000000	4.813065	0.457577
C	0.000000	-4.813065	0.457577
N	0.000000	6.067939	0.030487
N	0.000000	-6.067939	0.030487
H	0.000000	0.000000	1.241288
H	0.000000	1.263096	-1.569624
H	0.000000	-1.263096	-1.569624
H	0.000000	2.354078	1.307718
H	0.000000	-2.354078	1.307718
H	0.000000	3.805047	-1.419354
H	0.000000	-3.805047	-1.419354
H	0.000000	4.694589	1.536243
H	0.000000	-4.694589	1.536243
H	0.000000	6.288701	-0.950612
H	0.000000	-6.288701	-0.950612
H	0.000000	6.836633	0.675481
H	0.000000	-6.836633	0.675481

S7 Auxiliary Basis sets

#AUXILIARY BASIS SET: (8s, 8p, 8d)

H	S	0.100000000000000000	1.00000
H	S	0.2258782763143732	1.00000
H	S	0.5102099571075233	1.00000
H	S	1.1524534566987763	1.00000
H	S	2.6031420033166071	1.00000
H	S	5.8799322871069952	1.00000
H	S	13.2814896985695814	1.00000
H	S	30.00000000000000071	1.00000
H	P	0.100000000000000000	1.00000
H	P	0.2258782763143732	1.00000
H	P	0.5102099571075233	1.00000
H	P	1.1524534566987763	1.00000
H	P	2.6031420033166071	1.00000
H	P	5.8799322871069952	1.00000
H	P	13.2814896985695814	1.00000
H	P	30.00000000000000071	1.00000
H	D	0.100000000000000000	1.00000
H	D	0.2258782763143732	1.00000
H	D	0.5102099571075233	1.00000
H	D	1.1524534566987763	1.00000
H	D	2.6031420033166071	1.00000

H	D	5.8799322871069952	1.00000
H	D	13.2814896985695814	1.00000
H	D	30.0000000000000071	1.00000
#AUXILIARY BASIS SET: (8s, 8p, 8d)			
C	S	0.0100000000000000	1.00000
C	S	0.0769666979406701	1.00000
C	S	0.5923872591890347	1.00000
C	S	4.5594091241903856	1.00000
C	S	35.0922664849496471	1.00000
C	S	270.0935874600619400	1.00000
C	S	2078.8211561750540568	1.00000
C	S	15999.9999999999890861	1.00000
C	P	0.0100000000000000	1.00000
C	P	0.0769666979406701	1.00000
C	P	0.5923872591890347	1.00000
C	P	4.5594091241903856	1.00000
C	P	35.0922664849496471	1.00000
C	P	270.0935874600619400	1.00000
C	P	2078.8211561750540568	1.00000
C	P	15999.9999999999890861	1.00000
C	D	0.0100000000000000	1.00000
C	D	0.0769666979406701	1.00000
C	D		

	0.5923872591890347	1.00000
C D		
	4.5594091241903856	1.00000
C D		
	35.0922664849496471	1.00000
C D		
	270.0935874600619400	1.00000
C D		
	2078.8211561750540568	1.00000
C D		
	15999.9999999999890861	1.00000

#AUXILIARY BASIS SET: (8s, 8p, 8d)

N S		
	0.010000000000000000	1.00000
N S		
	0.0809813769781381	1.00000
N S		
	0.6557983417275318	1.00000
N S		
	5.3107452733075098	1.00000
N S		
	43.0071465012580560	1.00000
N S		
	348.2777943572392587	1.00000
N S		
	2820.4015357958055574	1.00000
N S		
	22839.9999999999818101	1.00000
N P		
	0.010000000000000000	1.00000
N P		
	0.0809813769781381	1.00000
N P		
	0.6557983417275318	1.00000
N P		
	5.3107452733075098	1.00000
N P		
	43.0071465012580560	1.00000
N P		
	348.2777943572392587	1.00000
N P		
	2820.4015357958055574	1.00000
N P		
	22839.9999999999818101	1.00000

N	D	0.010000000000000000	1.00000
N	D	0.0809813769781381	1.00000
N	D	0.6557983417275318	1.00000
N	D	5.3107452733075098	1.00000
N	D	43.0071465012580560	1.00000
N	D	348.2777943572392587	1.00000
N	D	2820.4015357958055574	
N	D	22839.9999999999818101	

References

- (1) Dunning, T. H. *J. Chem. Phys.* **1989**, *90*, 1007–1023.
- (2) Blase, X.; Attaccalite, C.; Olevano, V. *Phys. Rev. B* **2011**, *83*, 115103.
- (3) Blase, X.; Attaccalite, C. *Appl. Phys. Lett.* **2011**, *99*, 171909.
- (4) Cherkes, I.; Klaiman, S.; Moiseyev, N. *Int. J. Quant. Chem.* **2009**, *109*, 2996–3002.
- (5) Jacquemin, D.; Zhao, Y.; Valero, R.; Adamo, C.; Ciofini, I.; Truhlar, D. G. *J. Chem. Theory Comput.* **2012**, *8*, 1255–1259.